J. Biochem. **134**, 683–690 (2003)
DOI: 10.1093/jb/mvg193

Effect of Nitration on the Activity of Bovine Erythrocyte Cu,Zn-Superoxide Dismutase (BESOD) and a Kinetic Analysis of Its Dimerization-Dissociation Reaction as Examined by Subunit Exchange between the Native and Nitrated BESODs

Hiroshi Oneda and Kuniyo Inouye*

Division of Food Science and Biotechnology, Graduate School of Agriculture, Kyoto University, Sakyo-ku, Kyoto 606-8502

Received June 3, 2003; accepted August 27, 2003

Bovine erythrocyte Cu,Zn-superoxide dismutase (BESOD) is a dimeric enzyme composed of identical subunits associated through unusually strong non-covalent interactions. The state of the unique tyrosyl residue (Tyr 108) of BESOD was examined, and the kinetics of subunit exchange was studied using Tyr 108 as a probe. UV-absorption difference spectra demonstrate that Tyr 108 is exposed to the solvent, and that the accessibilities to ethanol, ethylene glycol, and polyethylene glycol 600 are 53.5, 52.0, and 44.6%, respectively. Tyr 108 was fully nitrated by tetranitromethane. The pK_a values of the phenolic hydroxyl group of native and nitrated Tyr 108 were determined to be 11.3 and 7.9, whereas those of model compounds, L-tyrosine and 3-nitro-L-tyrosine, are 9.8 and 6.8, respectively. When the native and nitrated BESODs of an equal concentration were mixed, the hybrid dimer was formed. From the amount of hybrid dimer formed, the rate constant (k_{-1}) of the subunit dissociation at pH 7.8, 25°C was assessed to be $(4.17 \pm 0.13) \times 10^{-6}$ s^{-1}. The activation energy of the subunit dissociation at pH 7.8 was determined to be 117 ± 4 kJ·mol^{-1}. The k_{-1} value remains constant at BESOD concentrations ranging from 0.62 to 6.8 μM and at pH ranging from 6.0 to 10.0, but increased remarkably with a decrease in the dielectric constant of the reaction mixture. It is suggested that hydrophobic interaction may play a significant role in the subunit interaction.

Key words: Cu,Zn-superoxide dismutase, difference spectrum, nitration, subunit exchange, subunit interaction.

Abbreviations: BESOD, bovine erythrocyte Cu,Zn-superoxide dismutase; EtOH, ethanol; EG, ethylene glycol; PEG 600, polyethylene glycol 600; MtOH, methanol; *N*-Ac-Tyr-NH_2, *N*-acetyl-l-tyrosine amide; TNM, tetranitromethane; XaNa, xanthine sodium salt; XOD, xanthine oxidase.

Superoxide dismutase (SOD) [EC 1.15.1.1] catalyzes the dismutation of the superoxide anion radical (O_2^-) into molecular oxygen and hydrogen peroxide. The enzyme is believed to take part in the cellular defense mechanism against the toxic effect of oxygen radicals (*1*).

The copper- and zinc-containing superoxide dismutase from bovine erythrocytes (BESOD) is a homodimer with the molecular weight of 32,000 (*1–4*). Two identical subunits composed of an antiparallel eight-stranded β-barrel with Greek key topology, three external loops, a catalytic copper, and a structural zinc are associated through unusually strong non-covalent interactions (*4*, *5*), but no cooperativity between the two subunits is observed in the activity (*6*). The dimer is related by a non-crystallographic 2-fold axis, and the contact comprising about 9% of total external surface of each subunit includes both hydrophobic and hydrophilic interactions involving the N and C termini, the first and last pair of β strands, and two loop regions (*5*).

*To whom correspondence should be addressed. Tel: +81-75-753-6266, Fax: +81-75-753-6265, E-mail: inouye@kais.kyoto-u.ac.jp

BESOD is also characterized by unusual stability and has a conformational melting temperature T_m of 83–104°C (*7–9*). Instead of some disagreements in the T_m values observed, these values are among the highest values so far reported for proteins. BESOD remains active in 8 M urea (*10*), is not dissociated into subunits even by 4% sodium dodecyl sulfate (SDS) (*11*), and is only gradually denatured in the presence of 6 M guanidine hydrochloride plus EDTA (*4*, *11–13*). In this context, interest in the subunit interactions led to several studies of the effects of urea on the activity and subunit structure of Cu,Zn-SODs (*14–18*). On the other hand, the engineered monomeric human Cu,Zn-SODs produced by replacing two hydrophobic residues located in the contact region of the subunits were shown to have much lower activities than that of the native enzyme (*19–21*). The significance of the stable dimeric structure and the structure-function relationship of Cu,Zn-SOD have not been clearly defined.

Each subunit of BESOD contains a unique tyrosyl residue (Tyr 108) near the contact region, and these are expected to be good probes to explore the nature of the stable dimeric structure of BESOD. In this paper, we describe the state of Tyr 108 as investigated by UV-

absorption difference spectroscopy, nitration with tetranitromethane (TNM), and spectrometric titration of pH-dependent ionization. The kinetics of the subunit exchange between the native and nitrated BESODs is also described, as well as the effects of temperature, enzyme concentration, pH, and dielectric constant of the reaction mixture on the subunit interaction. Evidence of the nature of the protein-protein interactions of the BESOD subunits is also provided.

MATERIALS AND METHODS

Materials—Bovine erythrocyte Cu,Zn-superoxide dismutase (BESOD) was purified according to the methods reported by McCord and Fridovich (*1*) with some modifications (*22*). The contents of Cu and Zn in 15,700 g BESOD were 0.98 and 0.96 g-atom, respectively, by flameless atomic absorption analyses. The concentrations of BESOD were determined by the Lowry method using bovine serum albumin (BSA) as a standard (*23*). The specific activity of the preparation was 3,600 units/mg according to the method of McCord and Fridovich (*1*). *N*-Acetyl-L-tyrosine amide (*N*-Ac-Tyr-NH_2) (Lot V2R6714), tetranitromethane (TNM) (Lot FFP209), xanthine sodium salt (XaNa) (Lot 7980) were purchased from Nacalai Tesque (Kyoto). Buttermilk xanthine oxidase (XOD) (Lot SAH7206), ethanol (EtOH), ethylene glycol (EG), and polyethylene glycol (PEG) 600 (average molecular weight: 600) were from Wako Pure Chemicals (Osaka). 3-Nitro-L-tyrosine (Lot TG10309TG) was from Aldrich Chemicals (Milwaukee, WI). Sephadex G-15 (Lot 12849) was from Pharmacia Fine Chemicals (Uppsala). Horse heart cytochrome c (Type III, Lot 118F8060) was from Sigma (St. Louis, MO).

Superoxide Dismutase (SOD) Assay—The SOD activity was measured according to the method of McCord and Fridovich (*1*). The assay was performed with a Shimadzu UV-VIS recording spectrophotometer UV-2200 in 3.01 ml of 50 mM potassium phosphate buffer (pH 7.8) plus 0.1 mM EDTA (buffer A) in a 10-mm cell at 25°C. The reaction mixture contained 10 μM ferricytochrome c, 50 μM XaNa, and a sufficient activity of XOD to produce a rate of reduction of ferricytochrome c at 550 nm of 0.025 absorbance unit per min. Under these defined conditions, the amount of SOD required to inhibit the rate of reduction of cytochrome c by 50% (*i.e.*, to a rate of 0.0125 absorbance unit per min) is defined as 1 unit of activity. The reaction was started by adding 100 μl of the XOD solution to the mixture (2.91 ml) of other components.

UV-Absorption Difference Spectra—UV-absorption difference spectra obtained upon mixing BESOD with perturbants (EtOH, EG, or PEG 600) were measured in a 10-mm cell in buffer A at 25°C with 0.5-nm slit width (*24*, *25*). Two sets of matched cells were used in a double tandem cell system. Equal volumes of BESOD and perturbant solutions were mixed in a cell on the sample side. The BESOD and perturbant solutions were placed separately in the cells on the reference side. The concentrations of BESOD and perturbants (0–20%, v/v) were adjusted so as to be the same on both the sample and reference sides. Difference spectra of a tyrosine model compound, *N*-Ac-Tyr-NH_2, were measured in place of BESOD.

Nitration of BESOD—Nitration was carried out by the addition of tetranitromethane (TNM) dissolved in MeOH to BESOD in buffer A. The BESOD and TNM concentrations in the reaction mixture were 30.4 μM and 0.336–30.2 mM, respectively. The reaction mixture was kept at 25°C for 1 h, and the reaction was terminated by passing the mixture through a Sephadex G-15 column [size: 1 cm (inner diameter) × 8 cm] equilibrated with buffer A. The degree of nitration was determined from the absorbance at 275 and 381 nm using the molar absorption values for *N*-acetyl-3-nitro-L-tyrosine of 4,000 and 2,200 $M^{-1}\cdot cm^{-1}$, respectively (*26–28*). The purity and molecular mass of the nitrated BESOD's was examined by gel-filtration HPLC on a TSKgel $G3000SW_{XL}$ column [size: 7.8 mm (inner diameter) × 30 cm] (Tosoh, Tokyo) in 20 mM Tris-HCl buffer (pH 7.8) (buffer B) at 25°C, at a concentration of 3.4 μM.

Spectrophotometric Titration—The spectrophotometric titration of tyrosine was performed by measuring the decrease in fluorescence that accompanies ionization (*29*). Four molar sodium hydroxide or hydrochloric acid was added to the BESOD or *N*-Ac-Tyr-NH_2 solutions, and the pH value of the solution and the fluorescence intensity at 306 nm with excitation at 275 nm were measured. The concentrations of BESOD and *N*-Ac-Tyr-NH_2 were 19.5 and 30.9 μM, respectively. In the same way, the titration of nitrotyrosine was performed by measuring the increase in absorbance at 428 nm that accompanies ionization (*26*). The concentrations of the nitrated BESOD and 3-nitro-L-tyrosine were 31.4 and 190 μM, respectively.

High-Performance Liquid Chromatography (HPLC)—The HPLC apparatus, composed of a solvent-delivery system CCPM, a UV monitoring system UV-8010, a computer-control system PX-8010, a degasser SD-8023, and a column oven CO-8020, was purchased from Tosoh (Tokyo). Anion-exchange HPLC was performed on a Mono Q HR 5/5 column [size: 5 mm (inner diameter) × 50 mm] (Pharmacia, Uppsala, Sweden) equilibrated with 20 mM borate buffer (pH 10.0), and eluted by a linear gradient from 50 to 200 mM NaCl at a flow-rate of 0.5 ml/min over 40 min from the beginning of the elution (time zero) at 25°C. A sample loop of 50 μl was used throughout this study, and the elution was monitored by absorbance at 260 nm.

Kinetic Studies of Subunit Exchange—Equal concentrations of native and nitrated BESOD were mixed in buffer B. At various incubation times, 50 μl of the sample was taken out and immediately analyzed by anion-exchange HPLC. Hybrid dimer formation, if it occurred,

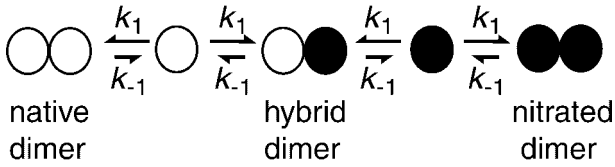

Fig. 1. **Reaction scheme of the subunit exchange between native and nitrated BESODs.** k_1 and k_{-1} are the rate constants of subunit association and dissociation, respectively. Open and solid circles represent the native and nitrated BESOD monomer, respectively.

was quantified from peak areas at each time point. Assuming that the rate constants of subunit dissociation and association are not affected by the nitration of Tyr 108, the reaction is represented as shown in Fig. 1, and the ratio of the amounts of native dimer, hybrid dimer, and nitrated dimer must be 1:2:1 at equilibrium. The time-dependence of the three dimer species is expressed in the following equations (*30*):

$$\frac{d[AA]}{dt} = k_1[A]^2 - k_{-1}[AA] \quad (1)$$

$$\frac{d[BB]}{dt} = k_1[B]^2 - k_{-1}[BB] \quad (2)$$

$$\frac{d[AB]}{dt} = 2k_1[A][B] - k_{-1}[AB] \quad (3)$$

where A and B represent the subunits or monomeric forms of the native and nitrated BESOD, respectively. Thus, AA and BB represent homodimers of native and nitrated BESOD, respectively, and AB is a heterodimer composed of A and B subunits. k_1 and k_{-1} are the rate constants of the association of the subunits into dimers and the dissociation of the dimer into subunits, respectively. The concentrations of the respective species at time t are expressed by brackets [ ]. The initial concentrations are expressed by brackets with a suffix zero, as $[\ ]_0$. Assuming that $[AB]_0 = 0$, $[A] \ll [AA]$, and $[B] \ll [BB]$, the total concentration of the three species of dimeric BESOD is expressed as:

$$[AA] + [BB] + [AB] = [AA]_0 + [BB]_0 \quad (4)$$

Under the initial condition of $[AA]_0 = [BB]_0$, the concentration of the hybrid dimer, AB, is shown by

$$[AB] = [AA]_0\{1 - \exp(-k_{-1} \cdot t)\} \quad (5)$$

The ratio of hybrid dimer formation is,

$$\frac{[AB]}{[AA] + [AB] + [BB]} = \frac{1 - \exp(-k_{-1} \cdot t)}{2} \quad (6)$$

Thus, the rate constant of subunit dissociation can be determined so as to fit experimental data to Eq. 6, using the least-squares regression method (*31*).

Thermodynamic Analysis of the Dissociation of BESOD—The activation energy (E_a) of the dissociation of BESOD was determined from the slope ($-E_a/R$) of the Arrhenius plots of k_{-1} against $1/T$, and the activation parameters of the dissociation were determined according to the following equations (*32*):

$$\Delta G^{\ddagger} = -RT\left(\ln k_{-1} - \ln\frac{k_B T}{h}\right) \quad (7)$$

$$\Delta H^{\ddagger} = Ea - RT \quad (8)$$

$$\Delta S^{\ddagger} = \frac{(\Delta H^{\ddagger} - \Delta G^{\ddagger})}{T} \quad (9)$$

where k_B, h, and R are the Boltzman, Plank, and gas constants, respectively, and T is the temperature shown in Kelvin.

Evaluation of the Dielectric Constant of the Reaction Mixture—The dielectric constant (D) of the reaction mixture was estimated by the following equation (*33–35*):

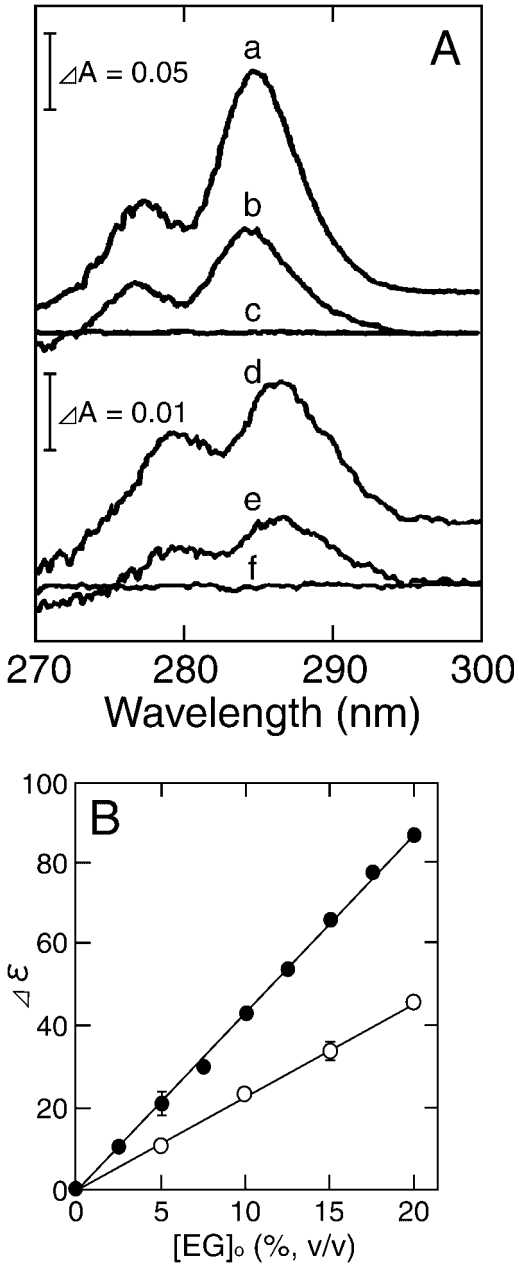

Fig. 2. **UV-absorption difference spectra of BESOD.** Panel A: UV-absorption difference spectra observed upon mixing of *N*-Ac-Tyr-NH_2 (a–c) or BESOD (d–f) with EG. The concentrations of *N*-Ac-Tyr-NH_2 and BESOD were 1.36 mM and 155 μM, respectively. The concentrations of EG were 0% (c, f), 10% (b, e), and 20% (a, c), respectively. The spectra were measured in buffer A at 25°C. Panel B: Dependence of the molar absorptivity difference ($\Delta\varepsilon\lambda$) on the concentration of EG. The molar absorptivity differences, $\Delta\varepsilon_{284.5}$ of *N*-Ac-Tyr-NH_2 (solid circles) and $\Delta\varepsilon_{286.5}$ of BESOD on a monomer basis (open circles), were plotted against the concentration of EG.

$$D = f_w \cdot D_w + f_a \cdot D_a \quad (10)$$

where f_w and f_a are the volume fractions of the water and alcohol, respectively (and thus $f_w + f_a = 1$), and D_w and D_a are the dielectric constants of the water and alcohol, respectively.

Table 1. **Molar absorption difference (Δελ) of *N*-Ac-Tyr-NH_2 and BESOD.**[a]

Perturbant	Δελ (M^{-1}·cm^{-1})/[perturbant] (%, v/v)		Accessibility(%)
	N-Ac-Tyr-NH_2[b]	BESOD[c]	
EtOH[d]	4.30 ± 0.10	2.25 ± 0.04	52.3
EG[e]	4.35 ± 0.04	2.26 ± 0.04	52.0
PEG 600[f]	10.4 ± 0.2	4.64 ± 0.08	44.6

[a]50 mM phosphate buffer (pH 7.8) plus 0.1 mM EDTA, 25°C. [b]λ = 284.5 nm. [c]λ = 286.5 nm. [d]EtOH, ethanol. [e]EG, ethylene glycol. [f]PEG 600, polyethylene glycol 600.

RESULTS

UV-Absorption Difference Spectra—UV-absorption difference spectra were obtained upon the mixing of *N*-Ac-Tyr-NH_2 or BESOD with EG (Fig. 2A). Two peaks were observed in the difference spectra with *N*-Ac-Tyr-NH_2 at 277.0 and 284.5 nm. BESOD showed difference spectra similar to those observed with *N*-Ac-Tyr-NH_2, with peaks at 279.5 and 286.5 nm. The tyrosyl residue alone might contribute to the difference spectra above 275 nm, because BESOD has no tryptophyl residue, and the contribution of phenylalanyl residues (4 residues per subunit) to the difference spectra is almost negligible. The molar absorption difference (Δελ) of *N*-Ac-Tyr-NH_2 at 284.5 nm and that of BESOD at 286.5 nm increased linearly with increasing EG concentration from 0 to 20% (v/v) (Fig. 2B). Assuming that *N*-Ac-Tyr-NH_2 is fully accessible to the solvent, the accessibility of Tyr 108 to EG can be estimated from the ratio of the slopes obtained with BESOD to that obtained with *N*-Ac-Tyr-NH_2, and was estimated to be 52.0%. Similar plots were obtained with EtOH and PEG 600, and the parameters are summarized in Table 1.

Nitration of BESOD—The nitration of BESOD was carried out by the addition of TNM dissolved in MeOH to BESOD in buffer A at 25°C, for 1 h (Fig. 3). Under these conditions, a 700-fold molar excess of TNM was required to achieve the maximal nitration, which corresponds to 1.9 nitrotyrosyl residues/mole BESOD dimer. The nitrated BESOD showed almost the same activity (3,500 ± 260 units/mg protein) as that of the native BESOD. The native and nitrated BESODs at a concentration of 3.4 μM eluted together as a single peak in gel-filtration HPLC on a TSKgel G3000SW_{XL} in buffer B (data not shown). This suggests that both BESODs are dimers with a molecular mass of 32.0 kDa.

Spectrometric Titration—The pK_a values of *N*-Ac-Tyr-NH_2 and Tyr 108 in the native BESOD were determined to be 9.8 and 11.3, respectively. On the other hand, the pK_a values of 3-nitro-L-tyrosine and Tyr 108 in the nitrated BESOD (namely, the nitrated Tyr 108) were determined to be 6.8 and 7.9, respectively. It is suggested that the nitrated BESOD dimer carries two extra negative charges at pH 10.0 in comparison with the native dimer based on the difference in the pK_a of Tyr 108 in the native and nitrated BESODs.

Anion-Exchange HPLC Analyses of BESOD—The native and nitrated BESODs at an equal concentration (3.4 μM) were mixed and incubated for various periods in buffer B at 45°C. The effect of the incubation time on the elution patterns of the BESODs in anion-exchange HPLC was examined (Fig. 4). Before examining the effect, the native and nitrated BESODs were applied separately to the anion-exchange HPLC to confirm their elutions as single peaks at 18.2 and 33.2 min, respectively (data not shown). This suggests that dissociation or aggregation of the BESOD dimers might not occur during HPLC. The difference in the retention time might be due to the dif-

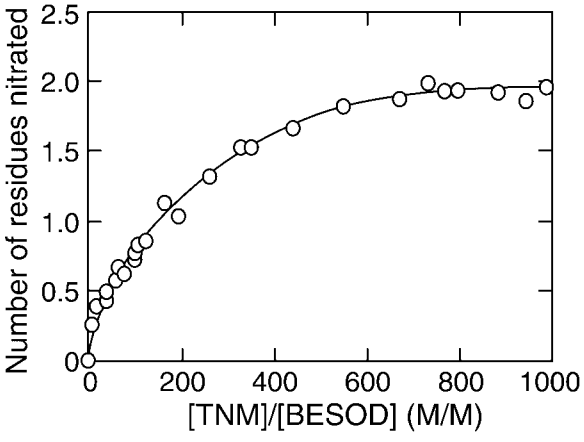

Fig. 3. **Nitration of BESOD with tetranitromethane (TNM).** Nitration of BESOD was carried out in buffer A at 25°C for 1 h. The concentration of BESOD was 30.4 μM.

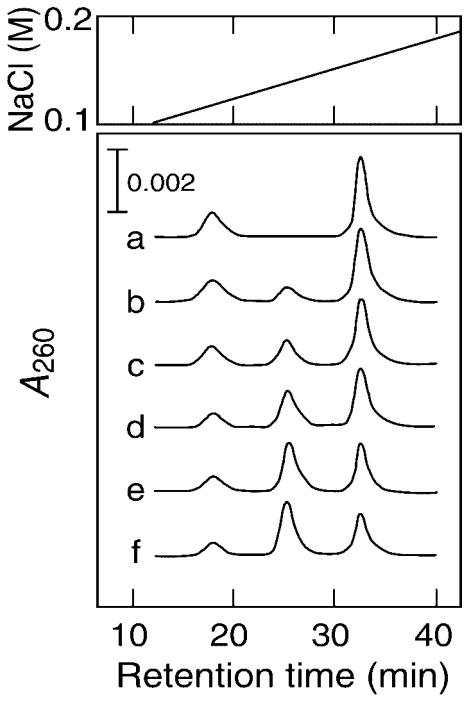

Fig. 4. **Time-dependence of the subunit exchange between native and nitrated BESODs as followed by anion-exchange HPLC.** The native and nitrated BESODs at equal concentrations (3.4 μM) were mixed in buffer B at 45°C and incubated for the period indicated. Aliquots (50 μl) of the mixture solution were collected at various times and immediately subjected to HPLC on a Mono Q column equilibrated with 20 mM borate buffer (pH 10.0) at 25°C. The column was eluted with a linear gradient from 50 to 200 mM NaCl at a flow-rate of 0.5 ml/min over 40 min. The incubation times were 0 (a), 20 (b), 84 (c), 189 (d), 325 (e), and 605 min (f).

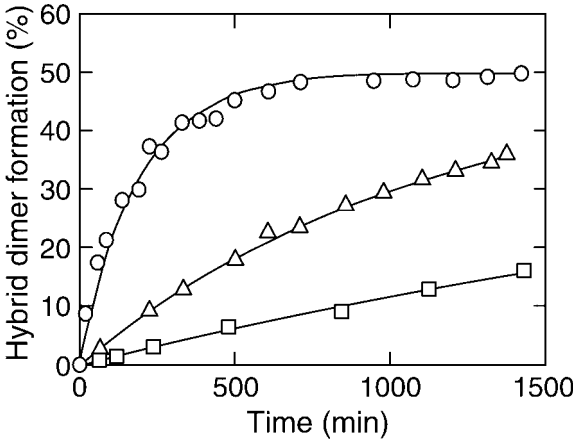

Fig. 5. **Time course of the formation of hybrid dimers of native and nitrated BESODs.** The native and nitrated BESODs at equal concentrations (3.4 μM) were mixed in buffer B at 25 (squares), 37 (triangles), and 45°C (circles) for the time indicated. The rate constants of subunit dissociation at 25, 37, and 45°C were determined to be $(4.17 \pm 0.13) \times 10^{-6}$, $(1.50 \pm 0.04) \times 10^{-5}$, and $(7.69 \pm 0.28) \times 10^{-5}$ s^{-1}, respectively.

ference in the net charge between the native and nitrated BESOD dimers. When the incubation time of the mixture was zero, two peaks were observed at 18.2 and 33.2 min, suggesting that the native and nitrated BESOD dimers eluted independently. Equal concentrations of the native and nitrated BESODs were mixed in buffer B and incubated for appropriate periods up to 605 min at 45°C. The mixtures were then analyzed on the same column. A new peak appeared at an elution time of 25.8 min, just in the middle between the native and nitrated dimers, and its height increased with increasing incubation time. This peak was attributed to the hybrid dimer carrying one extra negative charge in comparison with the native dimer. The ratio of the molar absorption coefficient at 260 nm of the nitrated BESOD to that of the native enzyme was determined to be 2.9 at pH 10.0. Therefore, when the reaction reached an equilibrium at t = 605 min, the molar ratio of the dimer species of the native, hybrid, and nitrated dimers was determined to be 1:2:1. No hybrid dimer peak was detected at time zero, indicating that subunit exchange during HPLC is negligible.

Thermodynamic Analysis of Subunit Exchange—Figure 5 shows the time courses for the formation of the hybrid dimer in buffer B at 25, 37, and 45°C. The solid lines are theoretical curves best-fitted to Eq. 7 by the least-squares regression method, and the rate constants (k_{-1}) of the subunit dissociation at 25, 37, and 45°C were determined to be $(4.17 \pm 0.13) \times 10^{-6}$, $(1.50 \pm 0.04) \times 10^{-5}$, and $(7.69 \pm 0.28) \times 10^{-5}$ s^{-1}, respectively. The k_{-1} values obtained at various temperatures were plotted according to the Arrhenius equation (Fig. 6). The activation energy (E_a) of the subunit dissociation at pH 7.8 was determined to be 117±4 kJ·mol^{-1}. The Gibbs free energy of activation ($\Delta G^{\ddagger}$), enthalpy of activation ($\Delta H^{\ddagger}$), and entropy of activation ($\Delta S^{\ddagger}$) at pH 7.8, 25°C were calculated to be 104 ± 0 kJ·mol^{-1}, 116 ± 4 kJ·mol^{-1}, and 40.3 ± 13.4 J·mol^{-1}·K^{-1}, respectively. The positive $\Delta H^{\ddagger}$ value suggests that the activation process is endothermic, and the positive $\Delta G^{\ddagger}$ and $\Delta S^{\ddagger}$ values suggest that the BESOD dimer might be converted to a more energy-rich and disordered state during the activation process.

Effects of the BESOD concentration, pH, and dielectric constant of the reaction mixture on k_{-1}—It was shown that the k_{-1} value is a constant 4×10^{-6} s^{-1} at BESOD concentrations ranging from 0.62 to 6.8 μM and at pH ranging from 6.0 to 10.0 (Figs. 7 and 8). The dielectric constant (D) of the reaction mixture was decreased by increasing the methanol (MeOH) or ethanol (EtOH) content in buffer B at 25°C. When k_{-1} was plotted against D, the dependence of k_{-1} on D was in good agreement in both cases. The k_{-1} value increased remarkably with a decrease in D, and was 15.2 times higher in the presence of 30% EtOH (D = 62.2) than in its absence (D = 78.3) (Fig. 9). This suggests that the dissociation of the BESOD dimer into subunits is promoted strongly by an increase

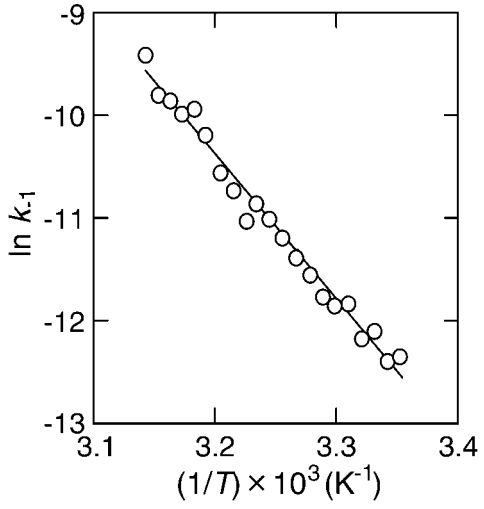

Fig. 6. **Arrhenius plots of the rate constant (k_{-1}) of the subunit dissociation.** The native and nitrated BESODs at equal concentrations (3.4 μM) were mixed in buffer B. The activation energy (E_a) was determined to be 117 ± 4 kJ·mol^{-1}.

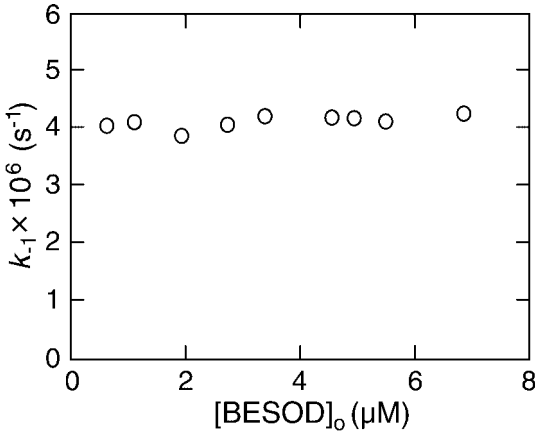

Fig. 7. **Dependence of the rate constant (k_{-1}) of subunit dissociation on BESOD concentration.** The native and nitrated BESODs at equal concentrations were mixed in buffer B at 25°C. $[BESOD]_o$ represents the total concentration of BESOD. (*i.e.*, $[BESOD]_o$ = [native BESOD]$_o$ + [nitrated BESOD]$_o$)

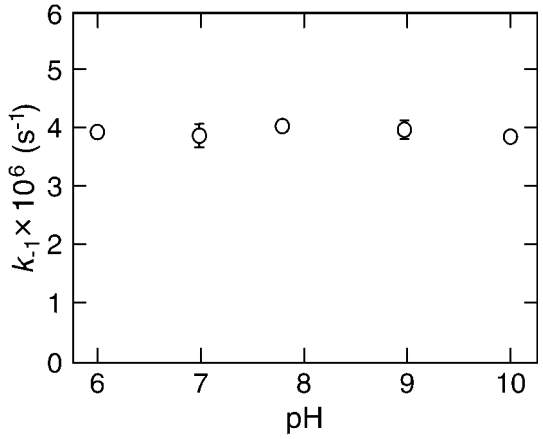

Fig. 8. **pH-Dependence of the rate constant (k_{-1}) of the subunit dissociation.** The native and nitrated BESODs at equal concentrations (2.7 μM) were mixed in 20 mM 3,3-dimethyl glutarate buffer (pH 6.0–7.0), Tris-HCl buffer (pH 7.0–9.0), or borate buffer (pH 9.0–10.0) at 25°C.

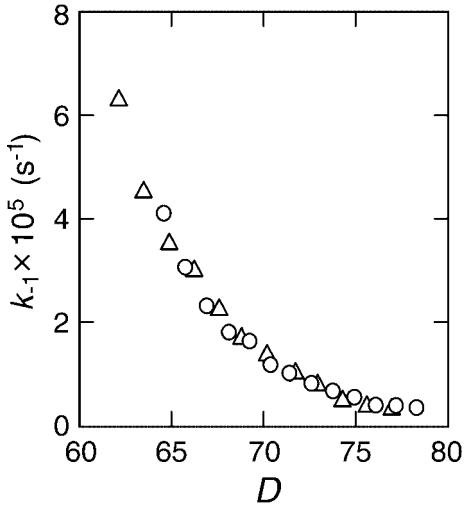

Fig. 9. **Dependence of the rate constant (k_{-1}) of subunit dissociation on the dielectric constant (D).** The native and nitrated BESODs at equal concentrations (2.7 μM) were mixed in buffer B plus methanol (circies) or ethanol (triangles) at 25°C. The concentrations of methanol and ethanol were in the range of 0–30%.

in the dielectric constant of the medium, while it is not affected by changes in BESOD concentration or pH.

DISCUSSION

UV-Absorption Difference Spectra of BESOD—The spectra of the residues located on the surface of proteins are usually perturbed by changes in the physical properties of the solvent (*e.g.*, refractive index, dielectric constant, solvent-solute interactions, *etc.*). Difference spectroscopic studies demonstrated that Tyr 108 is exposed in part to the solvent (Table 1). It should be noted that the accessibilities to EtOH, EG, and PEG 600 were in the range of 44.6–52.3% instead of the difference in the size of perturbants. The accessibility of Tyr 108 to water molecules was calculated from crystallographic data (*5*) to be 46 ± 9% by rolling a probe, the radius of which is 0.14 nm, around the accessible surface area of Tyr 108 and comparing it with the accessibility of Tyr in the extended Ala-Tyr-Ala tripeptide (*36*, *37*). However, based on the molecular sizes of water and the perturbants examined, it is suggested that the degree of exposure of Tyr 108 in solution might be much higher than that in the crystal.

Nitration of BESOD—TNM is a highly specific and selective reagent for nitrating tyrosyl residues in proteins, and BESOD was fully nitrated (1.9 nitrotyrosyl residues/mole BESOD dimer) with TNM. The nitrated BESOD showed almost the same activity as that of the native BESOD, suggesting that the nitration, if it is induced by peroxynitrite ($ONOO^-$) under pathological conditions, might not cause the inactivation of BESOD. The native and nitrated Tyr 108 showed abnormally high pK_a values of 11.3 and 7.9, which are 1.5 and 1.1 pH units higher than those of model compounds, respectively. From X-ray crystallographic analyses of native and nitrated BESODs (*5*, *38*), it is suggested that the abnormally high pK_a value of Tyr 108 may be due to adjacent hydrophobic side chains, and that nitration decreases the difference in pK_a between Tyr 108 and the model compound by 0.4 pH units. The state of the phenolic ring might be changed by nitration so that the nitrated phenolic ring may come into closer proximity with the carboxylate group of Glu 107. From this evidence, it is suggested that Tyr 108 is not in a free state on the surface of the subunit but in a considerably-strained state, although the nitration of Tyr 108 has no effects on the enzymatic activity and subunit interactions. These effects must be examined more precisely using spectrophotometric, calorimetric, and crystallographic measurements.

Subunit Exchange of BESOD—The three dimer species (*i.e.*, native, hybrid, and nitrated BESOD dimers) were clearly separated by anion-exchange HPLC. With sufficient incubation after mixing the native and nitrated BESOD dimers, the ratio of their amounts reached 1:2:1 at equilibrium. This ratio suggests strongly that the monomer-dimer equilibrium is not affected by nitration. The rate constant (k_{-1}) of subunit dissociation under the standard assay conditions (pH 7.8, 25°C), was determined to be $(4.17 \pm 0.13) \times 10^{-6}$ s^{-1}. However, no free monomer was detectable under the experimental conditions used, and thus the association rate and equilibrium constants could not be determined. Accordingly, the association rate constant was estimated by assuming that the subunit association could be diffusion-controlled and by taking into account the effective surface area for the subunit encounter. The rate constant of subunit encounter is assumed to be on the order of 10^9 $M^{-1}{\cdot}s^{-1}$ (*39*), and the effective surface area is about 9% of the total external surface of each subunit based on X-ray crystallographic data (*5*). Accordingly, the association rate constant is estimated to be on the order of 10^7 $M^{-1}{\cdot}s^{-1}$. The equilibrium constant (K_d) and Gibbs free energy change of subunit dissociation were estimated to be on the order of 10^{-13} M and about 74.2 kJ·mol^{-1} at pH 7.8, 25°C.

A well-characterized protein proteinase inhibitor, *Streptomyces* subtilisin inhibitor (SSI), is a 23-kDa homodimer (*40–43*). The subunit dissociation rate constant of SSI has been determined to be 1.4×10^{-6} s^{-1} at

4°C (*30*), whereas that of BESOD at 4°C is 9.6×10^{-8} s^{-1}. On the other hand, the activation energy of subunit dissociation of human stem-cell factor has been determined to be 85.7 kJ·mol^{-1} at pH 4.5 (*44*), whereas that of BESOD at pH 7.8 is 117.0 kJ·mol^{-1}. These results suggest that BESOD subunits are associated through stronger interactions than other proteins so far reported.

The k_{-1} value was affected by neither the BESOD concentration (0.62–6.8 μM) nor pH (6.0–10.0). Under the standard assay condition at pH 7.8, 25°C, Tyr 108 of BESOD is not ionized, whereas that of nitrated BESOD is approximately half ionized because of its pK_a value of 7.9. However, k_{-1} was not affected by pH in the range from 6.0 to 10.0, indicating that the contribution of the extra negative charge in the nitrated Tyr 108 to subunit exchange is negligible. The k_{-1} value increased remarkably with a decrease in the dielectric constant (D) of the reaction medium, suggesting that hydrophobic interactions in the subunit contact region play a significant role in subunit association. On the other hand, the BESOD monomer is negatively charged at pH 7.8 because of the isoelectric point of 4.9–5.5 (*22*). Taking only electrostatic interactions into account, it is supposed that monomers repulse each other, and this repulsive electrostatic interaction is strengthened with a decrease in D. Thus, the decrease in D results in the promotion of subunit dissociation in terms of both hydrophobic and electrostatic interactions. Larsen *et al*. reported a visual survey of 136 homodimeric proteins with images that highlight the major structural features of each protein-protein interaction surface (*45*). One-third of the interfaces show a recognizable hydrophobic core, with a single large continuous, hydrophobic patch surrounded by a ring of intersubunit polar interactions. The remaining two-thirds of proteins show a varied mixture of small hydrophobic patches, polar interactions and water molecules scattered over the interfacial area. The scattered hydrophobic patches, each comprising 1–3 amino acids, do not dominate the character of the interface as in the case of the large, central, hydrophobic cores. In the case of Cu,Zn-SOD, which forms one of the smallest mixed interfaces, two hydrogen bonds, half a dozen hydrophobic contacts and a few water molecules comprise the entire interface. As it is reasonably considered that the energies (8–40 kJ/mol) for interactions between two hydrophobic groups are almost the same as the bond dissociation energies (4–20 kJ/mol) of hydrogen bonds in liquid water (*46*, *47*), it is supposed that hydrophobic interactions could be contributing to the subunit interaction of Cu, Zn-SOD more than hydrogen bonds. It should be noted that the dissociation rate of dimer BESOD into monomer subunits is not dependent on the BESOD concentration under the assay conditions [20 mM Tris-HCl buffer (pH 7.8)] used in this study (Fig. 7). On the other hand, the dissociation has been reported to be dependent on the protein concentration with [BESOD] existing as 50% dimers at about 10 μM. In this case, BESOD was incubated in 50 mM potassium phosphate buffer (pH 7.8) at 25°C for 1 h, and then applied to gel-filtration HPLC in 50 mM potassium phosphate buffer (pH 6.6) plus 0.3 M NaCl to observe the dissociation (*18*). This discrepancy might stem from the difference in the HPLC conditions, and suggests that the subunit interaction of BESOD may be sensitive not only to alcohols (Fig. 9) but also to salts. This complex character of the interaction may be a reflection of the mixed interface of small hydrophobic patches, hydrogen bonds, and water molecules in the subunit interface.

Here, it has been demonstrated that BESOD dimers exchange subunits spontaneously with other dimers, and that subunit dissociation is highly dependent on the temperature and dielectric constant of the reaction mixture. The dimerization-dissociation reaction of BESOD has been characterized by examining subunit exchange between native and nitrated BESODs, and provides insights into the nature of the protein-protein interaction between BESOD subunits. The methods used here for studying protein-protein specific interactions may be applicable to other protein systems, and the observations obtained here may be useful in revealing the nature and significance of dimeric proteins.

REFERENCES

1. McCord, J.M. and Fridovich, I. (1969) Superoxide dismutase. *J. Biol. Chem.* **244**, 6049–6055
2. Evans, H.J., Steinman, H.M., and Hill, R.L. (1974) Bovine Erythrocyte Superoxide dismutase: Isolation and characterization of tryptic, cyanogen bromide, and maleylated tryptic peptides. *J. Biol. Chem.* **249**, 7315–7325
3. Steinman, H.M., Naik, V.R., Abernethy, J.L., and Hill, R.L. (1974) Bovine erythrocyte superoxide dismutase: Complete amino acid sequence. *J. Biol. Chem.* **249**, 7326–7338
4. Abernethy, J.L., Steinman, H.M. and Hill, R.L. (1974) Bovine erythrocyte superoxide dismutase: Subunit structure and sequence location of the intrasubunit disulfide bond. *J. Biol. Chem.* **249**, 7339–7347
5. Tainer, J.A., Getzoff, E.D., Beem, K.M., Richardson, J.S., and Richardson, D.C. (1982) Determination and analysis of the 2Å structure of copper, zinc superoxide dismutase. *J. Mol. Biol.* **160**, 181–217
6. Malinowski, D.P. and Fridovich, I. (1979) Bovine erythrocyte superoxide dismutase: diazo coupling, subunit interactions, and electrophoretic variants. *Biochemistry* **18**, 237–244
7. Stellwagen, E. and Wilgus, H. (1978) in *Biochemistry of Thermophily* (Friedman, S.M., ed) pp. 223–232, Academic Press, New York
8. Lepock, J.R., Arnold, L.D., Torrie, B.H., Andrews, B., and Kruuv, J. (1985) Structural analyses of various Cu^{2+}, Zn^{2+}-superoxide dismutases by differential scanning calorimetry and Raman spectroscopy. *Arch. Biochem. Biophys.* **241**, 243–251
9. Roe, J.A., Butler, A., Scholler, D.M., Valentine, J.S., Marky, L., and Breslauer, K.J. (1988) Differential scanning calorimetry of Cu, Zn-superoxide dismutase, the apoprotein, and its zinc-substituted derivatives. *Biochemistry* **27**, 950–958
10. Malinowski, D.P. and Fridovich, I (1979) Subunit association and side-chain reactivities of bovine erythrocyte superoxide dismutase in denaturing solvents. *Biochemistry* **18**, 5055–5060
11. Forman, H.J. and Fridovich, I. (1973) On the stability of bovine superoxide dismutase. *J. Biol. Chem.* **248**, 2645–2649
12. Mach, H., Dong, Z., Middaugh, C.R., and Lewis, R.V. (1991) Conformational stability of Cu, Zn-superoxide dismutase, the apoprotein, and its zinc-substituted derivatives: Second-derivative spectroscopy of phenylalanine and tyrosine residues. *Arch. Biochem. Biophys.* **287**, 41–47
13. Mei, G., Rosato, N., Silvia, N., Jr., Rusch, R., Gratton, E., Savini, I., and Finazzi-Agro, A. (1992) Denaturation of human Cu/Zn superoxide dismutase by guanidine hydrochloride: A dynamic fluorescence study. *Biochemistry* **31**, 7224–7230

14. Marmocchi, F., Venardi, G., Bossa, F., Rigo, A., and Rotilio, G. (1978) Dissociation of Cu, Zn-superoxide dismutase into monomers by urea. *FEBS Lett.* **94**, 109–111
15. Bannister, J.V., Anastasi, A., and Bannister, W.H. (1978) Active subunits from superoxide dismutase. *Biochem. Biophys. Res. Commun.* **81**, 469–472
16. Kanematsu, S. and Asada, K. (1989) CuZn-superoxide dismutases in rice: Occurrence of an active, monomeric enzyme and two types of isozyme in leaf and non-photosynthetic tissues. *Plant Cell Physiol.* **30**, 381–391
17. Battistoni, A., Folcarelli, S., Gabbianelli, R., Capo, C., and Rotilio, G. (1996) The Cu, Zn superoxide dismutase from *Escherichia coli* retains monomeric structure at high protein concentration. *Biochem. J.* **320**, 713–716
18. Inouye, K., Osaki, A., and Tonomura, B. (1994) Dissociation of dimer of bovine erythrocyte Cu, Zn-superoxide dismutase and activity of the monomer subunit: Effects of urea, temperature, and enzyme concentration. *J. Biochem.* **115**, 507–515
19. Bertini, I., Piccioli, M., Viezzoli, M.S., Chiu, C.Y., and Mullenbach, G.T. (1994) A spectroscopic characterization of a monomeric analog of copper, zinc superoxide dismutase. *Eur. Biophys. J.* **23**, 167–176
20. Banci, L., Benedetto, M., Bertini, I., Del, Conte, R., Piccioli, M., and Viezzoli, M.S. (1998) Solution structure of reduced monomeric Q133M2 copper, zinc superoxide dismutase (SOD). Why is SOD a dimeric enzyme? *Biochemistry* **37**, 11780–11791
21. Ferraroni, M., Rypniewski, W., Wilson, K.S., Viezzoli, M.S., Banci, L., Bertini, I., and Mangani, S. (1999) The crystal structure of the monomeric human SOD mutant F50E/G51E/E133Q at atomic resolution. The enzyme mechanism revisited. *J. Mol. Biol.* **285**, 413–426
22. Inouye, K., Nakamura, K., Mitoma, Y., Matsumoto, M., and Igarashi, T. (1985) Application of a new ion exchanger TSK-GEL DEAE-5PW, to the purification of Cu, Zn-superoxide dismutase of bovine erythrocytes. *J. Chromatogr.* **327**, 301–311
23. Lowry, O.H., Rosebrough, N.J., Farr, A.L., and Randall, R.J. (1951) Protein measurement with the folin phenol reagent. *J. Biol. Chem.* **193**, 265–275
24. Herskovits, T.T. and Laskowski, M., Jr. (1962) Location of chromophoric residues in proteins by solvent perturbation. *J. Biol. Chem.* **237**, 2481–2492
25. Inouye, K., Tonomura, B., Hiromi, K., Sato, S., and Murao, S. (1977) The states of tyrosyl and tryptophyl residues in protein proteinase inhibitor (*Streptomyces* Subtilisin Inhibitor). *J. Biochem.* **82**, 1207–1215
26. Sokolovsky, M., Riordan, J.F., and Vallee, B.L. (1966) Tetranitromethane. A reagent for the nitration of tyrosyl residues in protein. *Biochemistry* **5**, 3582–3589
27. Goto, K., Takahashi, N., and Murachi, T. (1971) Chemical modification of tyrosyl residues of stem bromelain. *J. Biochem.* **70**, 157–164
28. Lee, S.-B., Inouye, K., Tonumura, B. (1997) The state of tyrosyl residue in thermolysin as examined by nitration and pH-dependent ionization. *J. Biochem.* **121**, 231–237
29. White, A. (1959) Effect of pH on fluorescence of tyrosine, tryptophan and related compounds. *Biochem. J.* **71**, 217–220
30. Akasaka, K., Fujii, S., Hayashi, F., Rokushika, S., and Hatano, H. (1982) A novel technique for the detection of dissociation-association equilibrium in highly associable macromolecular system. *Biochem. Internat.* **5**, 637–642
31. Sakoda, M. and Hiromi, K. (1976) Determination of the best-fit values of kinetic parameters of the Michaelis-Menten equation by the method of least squares with Taylor expansion. *J. Biochem.* **80**, 547–555
32. Dixon, M. and Webb, E.C. (1979) *Enzymes*, 3rd ed., pp. 164–182, Academic Press, New York
33. Mellan, I. (1959) in *Source Book of Industrial Solvents.* Vol. **3**, pp. 199–200, Van Nostrand Reinhold, London
34. Inouye, K., Lee, S.-B., Nambu, K., and Tonomura, B. (1997) Effects of pH, temperature, and alcohols on the remarkable activation of thermolysin by salts. *J. Biochem.* **122**, 358–364
35. Muta, Y. and Inouye, K. (2002) Inhibitory effects of alcohols on thermolysin activity as examined using a fluorescent substrate. *J. Biochem.* **132**, 945–951
36. Lee, B. and Richards, F.M. (1971) The interpretation of protein structures: Estimation of static accessibility. *J. Mol. Biol.* **55**, 379–400
37. Kabsch, W. and Sander, C. (1983) Dictionary of Protein secondary structure: Pattern recognition of hydrogen-bonded and geometrical features. *Biopolymers* **22**, 2577–2637
38. Smith, C.D., Carson, M., van der Woerd, M., Chen, J., Ischiripoulos, H., and Beckman, J.S. (1992) Crystal structure of peroxynitrite-modified bovine Cu, Zn superoxide dismutase. *Arch. Biochem. Biophys.* **299**, 350–355
39. Hiromi, K. (1979) *Kinetics of Fast Enzyme Reactions*, pp. 255–273, Halsted Press, New York
40. Inouye, K., Tonomura, B., Hiromi, K. (1979) The effect of sodium dodesyl sulfate on the structure and function of a proteinase inhibitor, *Streptomyces* subtilisin inhibitor. *Arch. Biochem. Biophys.* **192**, 260–269
41. Inouye, K., Tonomura, B., and Hiromi, K. (1979) Interaction of α-chymotrypsin and a protein proteinase inhibitor, *Streptomyces* subtilisin inhibitor. The formation of a ternary complex of *Streptomyces* subtilisin inhibitor, α-chymotrypsin, and proflavine. *J. Biochem.* **85**, 601–607
42. Inouye, K., Tonomura, B., and Hiromi, K. (1979) The interaction of tyrosyl residue and carboxyl groups in the specific interaction between *Streptomyces* subtilisin inhibitor and subtilisin BPN'. A chemical modification study. *J. Biochem.* **85**, 1115–1126
43. Inouye, K., Tonomura, B., and Hiromi, K. (1979) Further studies on the interaction between a protein proteinase inhibitor, *Streptomyces* subtilisin inhibitor, and thiolsubtilisin BPN′. *J. Biochem.* **85**, 1127–1134
44. Lu, H.S., Chang, W.C., Mendiaz, E.A., Mann, M.B., Langley, K.E., and Hsu, Y.R. (1995) Spontaneous dissociation-association of monomers of the human-stem-cell-factor dimer. *Biochem. J.* **305**, 563–568
45. Larsen, T.A., Olson, A.J., and Goodsell, D.S. (1998) Morphology of protein-protein interfaces. *Structure* **6**, 421–427
46. Fersht, A. (1985) *Enzyme Structure and Mechanism*, 2nd ed., pp. 293–310, W.H. Freeman and Company, New York
47. Creighton, T.E. (1993) *Proteins: Structure and Molecular Properties*, 2nd ed., pp. 337–344, W.H. Freeman and Company, New York